

# Force heterogeneities in particle assemblies: From order to disorder

Leonardo E. Silbert\*

*Department of Physics, Southern Illinois University, Carbondale, IL 62901, U.S.A.*

The effect of increasing structural disorder on the distribution of contact forces  $P(f)$ , inside three dimensional particle assemblies is systematically studied using computer simulations of model granular packings. Starting from a face-centred cubic array, where all contact forces are identical, an increasing number of defects is introduced into the assembly, after which the system is then allowed to relax into a new mechanically stable state. Three distinct protocols for imposing disorder are compared. A quantitative measure of the disorder is obtained from distributions of the coordination number and three-particle contact angle. The distribution of normal contact forces show dramatic qualitative changes with increasing disorder. In the regime where the disorder is relatively weak, the pressure and the lowest normal mode frequency scale approximately linearly in the coordination number, with distance from the crystalline state. These results for  $P(f)$  are discussed in the context of jamming phenomena in glassy and granular materials.

PACS numbers: 61.43.-j 83.80.Fg

Over the past decade or so it has come to light that the way the contact forces are distributed through a static pile of grains occurs in a rather inhomogeneous manner compared to that of an equilibrium liquid, even though the arrangement of the particles are similar in both cases [1]. Whereas many pairs of touching particles in a granular packing experience only a small force between them, others experience much larger forces. In fact, there are more of these high-force contacts than one might expect if a static packing of particles were truly representative of a snapshot of a thermodynamic system. What is becoming increasingly apparent, is that the properties of granular packings appear to share many similarities with amorphous, glassy phases of their atomic and colloidal counterparts [2]. Simply due to the fact that grains are easier to see than atoms, granular materials now hold a prominent role in studies of amorphous systems.

However, what has yet to be determined in detail is how the properties of a static packing depend on the arrangement of the particles. To date, most studies have focused on the two extreme cases of either, fully disordered particle packings, where there are no long-ranged correlations in the particle positions, or perfectly ordered arrays. Yet, it is not clear how the properties of a static packing change as the configuration is tuned from an ordered array to a disordered state. It is this type of order-disorder “transition” that is addressed here.

With the recent upsurge in the study of granular materials, several notable properties of particle packings have emerged. One of the most robust, and reproducible, features of a *disordered* grain pile, that sets it apart from more traditional crystalline solids, is the probability distribution function of contact forces  $P(f)$ , where  $f \equiv F / \langle F \rangle$  is the normal force  $F$  between two particles in contact, normalized by the configuration-averaged force  $\langle F \rangle$ . It has been shown experimentally, numeri-

cally, and by computer simulations, that  $P(f)$  for a disordered particle packing exhibits an exponential’ish [3] decay at forces  $f$ , greater (roughly twice) than the average force, and a peak or plateau at small forces (below half the average force) [4, 5, 6, 7, 8]. All of these studies suggest that  $P(f)$  is quite insensitive to system size as well dimensionality. Experiments on three dimensional packings [9] have reported that  $P(f)$  is surprisingly insensitive to the structure of the packing and particle properties (such as the friction coefficient). For softer, rubber particles there appears to be a cross-over to a power-law tail at high forces [10]. Granular dynamics simulations have shown that for disordered packings, properties such as friction and inelasticity, have only a subtle effect on  $P(f)$  [8], whereas geometrical features of the packing, such as coordination number, do depend quite sensitively on the parameters chosen [11]. Hard-sphere simulations of vacancy-diluted crystals show a depletion of small forces compared with disordered configurations [12].

As discussed above, disordered particle packings can exhibit a number of subtle differences. However, there is one extreme case that is well-defined. For a perfectly ordered, face-centred cubic (fcc), crystalline array, all particles have the same number of contact neighbours so that the coordination number is  $z = z_{\text{fcc}} \equiv 12$ , and experience the same contact forces,  $f = 1$ . The distributions of the coordination number  $P(z)$ , and contact forces  $P(f)$ , are thus known exactly,

$$\begin{aligned} P_{\text{fcc}}(z) &= \delta(z - z_{\text{fcc}}) \\ P_{\text{fcc}}(f) &= \delta(f - 1). \end{aligned} \quad (1)$$

Clearly, there is a need to extract which properties of a static array of particles are responsible for determining the way forces are distributed. For this reason, the work presented here provides a systematic study as to how structural disorder affects the distribution of forces inside three dimensional (3D) particle assemblies.

The computer experiments reported here are for a model system: three dimensional, frictionless and non-

---

\*Electronic address: lsilbert@physics.siu.edu

cohesive, soft-sphere packings, with periodic boundary conditions. Two particles are defined to be neighbours and interact through a purely-repulsive, short-range, potential:  $V(r) = k(d - r)^2$ , when their centre-centre separation  $r < d$ , where  $d$  is the sum of their radii, and  $V(r) = 0$ , otherwise. To create the particle configurations with varying amounts of disorder, a number of protocols were implemented:

- (i) In the first method,  $N = 16,384$  particles were arranged into a 3D, fcc array, slightly over-compressed to a packing fraction  $\phi = 0.742$ , just above that of a hard sphere fcc array,  $\phi_{\text{fcc}} = \sqrt{2}\pi/6$ , and with  $z = z_{\text{fcc}}$ . Disorder was introduced by randomly removing,  $0.005 < \delta N < 40\%$  of the particles. To remain at constant packing fraction, the system was then “quenched” to the same initial  $\phi = 0.742$ , using an energy minimization algorithm [13]. These are denoted *quenched packings*. The resulting changes in the final packings were then analysed. In the following figures, each data set for a particular  $\delta N$ , was averaged over 5 independent realisations.
- (ii) The second protocol was similar to the first, but instead of removing particles, particles chosen at random had their diameters reduced by 10%, before being re-quenched. In this case, the system was made increasingly bidisperse. In each of the two cases (i) and (ii), the same procedure was again repeated using quenched molecular dynamics, with  $N = 16384$  and  $N = 256,000$  particles.
- (iii) The final protocol used started with  $N = 32,000$  particles arranged into a fcc array at  $\phi_{\text{fcc}}$ , constrained in the vertical direction by flat base and a free, top surface, with periodic boundary conditions in the horizontal plane [11]. Disorder was then introduced by removing particles at random, then allowing the assembly to relax under gravity - *gravity sedimented packings*.

The various protocols introduced above create configurations which are, statistically, very similar. Most of the results presented here are for the quenched, frictionless packings of protocol (i). To clarify the following nomenclature, the configurations generated via protocols (i) and (ii) are labelled  $Cn$ , where  $n$  is an index indicating the amount of disorder. Larger  $n$  correspond to packings with more defects, either by removing particles as in (i), or changing the particle size, as in (ii). To provide a comparison, two amorphous packings (A1 and A2) were generated (at two different packing fractions as detailed below), using the same interaction potential.

The average coordination number  $z$ , and the three-particle contact angle  $\theta$ , quantify how the protocols generate configurations of varying disorder.  $\theta$  is defined as the angle subtended by particle  $i$  and two of its contact neighbours:  $\widehat{jik}$ . Figure 1 shows the evolution of the distributions  $P(z)$ . The different configurations are labelled

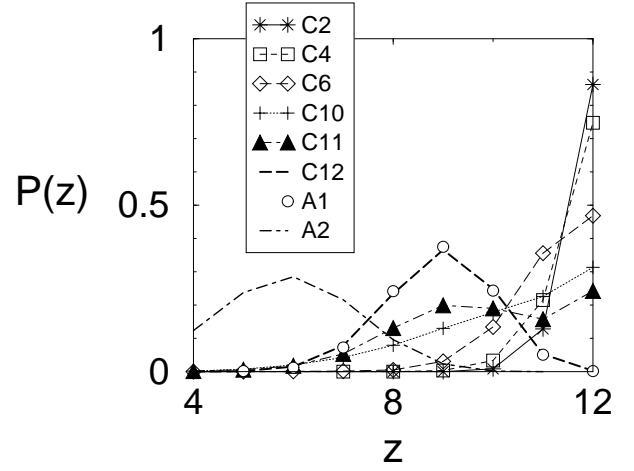


FIG. 1: Protocol (i): (a) Coordination number distributions  $P(z)$ , for different amounts of disorder introduced by removing a fraction,  $\delta N$ , of the particles. Increasing configuration label (C) corresponds to increasing disorder. The “A1” data is an amorphous packing generated from an initially random distribution of particles quenched to same  $\phi = 0.742$ . For comparison, the “A2” data is for an amorphous packing at random close packing,  $\phi = 0.64$ .

in increasing value according to the number of particles removed: configurations C[1-12] correspond to  $\delta N/N = (0.006, 0.012, 0.018, 0.024, 0.030, 0.06, 0.09, 0.12, 0.15, 0.18, 0.24, 0.36)$ . The “A1” system was generated from an initially random distribution of particles quenched to the same  $\phi = 0.742$ . The “A2” amorphous configuration is close to the random close packing point at  $\phi = 0.64$ .

Although the  $P(z)$  deviate from the fcc delta-function even for little disorder, the average coordination  $z$ , remain close to  $z_{\text{fcc}}$ . The deviation in coordination number from the initial crystal state quantitatively characterises the disorder. As shown in Fig. 2, for  $\delta N \ll N$ ,

$$\delta z \propto \delta N, \quad (2)$$

where  $\delta z \equiv z_{\text{fcc}} - z$ , is the change in the average coordination number relative to the initial crystal. Thus  $\delta z$  provides a convenient measure of how far away the final configuration is from the crystalline state. Hence, a *weakly* disordered regime can be roughly identified with configurations for which Eq. 2 applies, namely configurations C[1 – 7], for protocol (i).

Similarly, the distributions in the three-particle contact angle,  $P(\theta)$ , shown in Fig. 3, reflect the fact that protocol (i) induces only slight deviations from the fcc contact topology. Even up to C11, there are a significant fraction of three-particle collineations ( $\theta = 180^\circ$ ), whereas, for amorphous packings these become rare [14].

Visualisation of the force networks indicate that the forces are very sensitive to the imposed disorder. To illustrate this, Fig. 4 shows the averaged change in the pressure (normal stresses) between the initial crystal and final

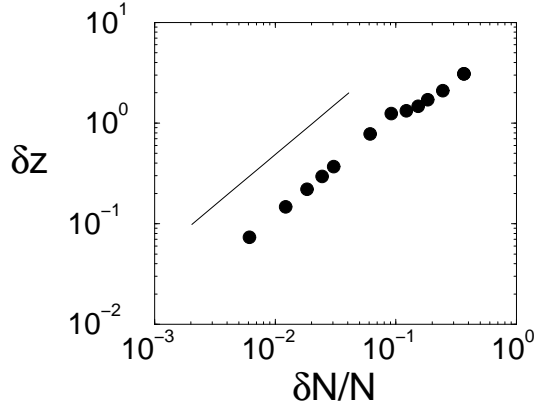


FIG. 2: Protocol (i): Relation between the number of defects  $\delta N$ , introduced into the packing, and the deviation in the coordination number  $\delta z$ , relative to the initial crystal structure. A weakly disordered regime can be identified where,  $\delta z \propto \delta N$ . Here, this corresponds to configurations  $C[1 - 7]$ .

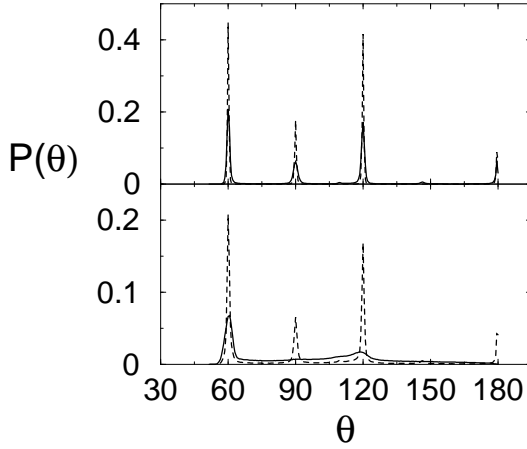


FIG. 3: Protocol (i): Three-particle contact angle distributions for, (top panel) C2 (dashed line) and C6 (full line), and (bottom) C11 (dashed) and C12 (full).

the configurations of two systems with different amounts of disorder.

The distribution of normal contact forces  $P(f)$  shown in Fig. 5 quantify the resulting changes in the force network. For a small fraction of defects, upto and including configuration C6, the region around the primary peaks in  $P(f)$  initially undergo Gaussian broadening from the original, fcc delta-function. Where the peak remains identifiable, the standard deviations  $s$ , of Gaussian fits to the primary  $P(f)$  peaks, grow as the location of the peaks  $f_{\text{peak}}$ , move to lower forces with increasing disorder. This is shown in the inset to Fig. 5(a). (Recall that for the fcc array,  $f_{\text{peak}}^{\text{fcc}} = 1$ .) In this regime, the  $P(f)$  develop additional features either side of  $f_{\text{peak}}$ , reflecting local force balance in the presence of local defects. These features correspond to the regime where Eq. 2 apply. As

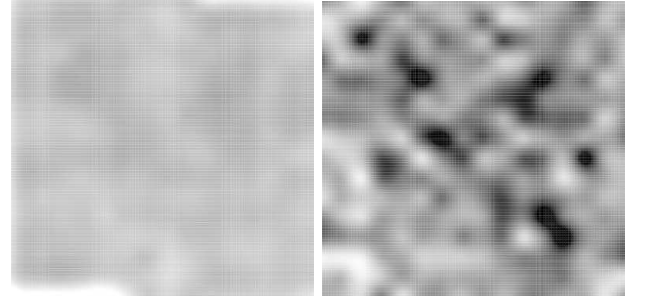


FIG. 4: Normal stress maps of the relative change in pressure between the initial crystal and the disordered packing. Each panel was averaged over 5 realisations. Left: Nearly ordered configuration (C2). Right: intermediate disorder (C11). Larger stress represented by darker shading. Same greyscale in both panels.

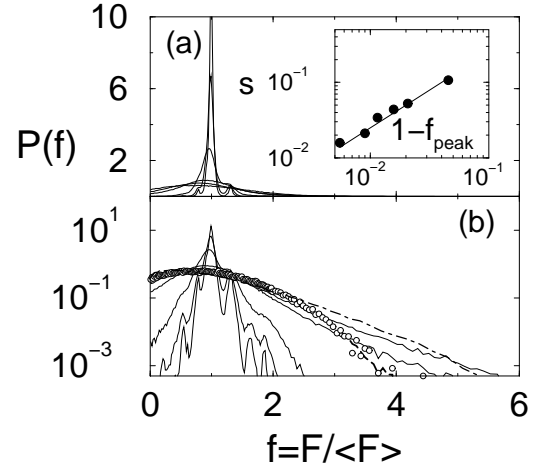


FIG. 5: Protocol (i): Distributions of normal contact forces  $P(f)$ , for varying disorder at fixed  $\phi = 0.742$ : (a) linear axes and (b) linear-log. In (b), the inner curve is for configuration C2 (thick solid line), extending outwards with increasing disorder, C4, C6, C8, C10, and C12 (thick dashed). The circles sitting on top of C12 is the data for the “A1” at  $\phi = 0.742$ . For comparison, the thick dash-dotted line is the “A2” data at  $\phi = 0.64$ . The inset to (a) shows the standard deviations  $s$ , of Gaussian fits to the  $P(f)$  peaks, growing linearly with the peak position  $f_{\text{peak}}$ , shifted relative to the fcc.

further disorder is introduced, the distributions become increasingly asymmetric; showing a dramatic increase in the number of very small forces and where the high- $f$  tails become increasingly broad (exponential) [15]. Thus, structure plays a crucial role in determining the heterogeneity of the force network in particle packings.

For small disorder, protocols (i) and (ii) generate configurations with properties that are almost indistinguishable. For more disorder, although the configurations generated via protocols (i) and (ii) have similar properties, there are a few noticeable differences. For this reason, the results for protocol (ii) are shown in Fig. 6.

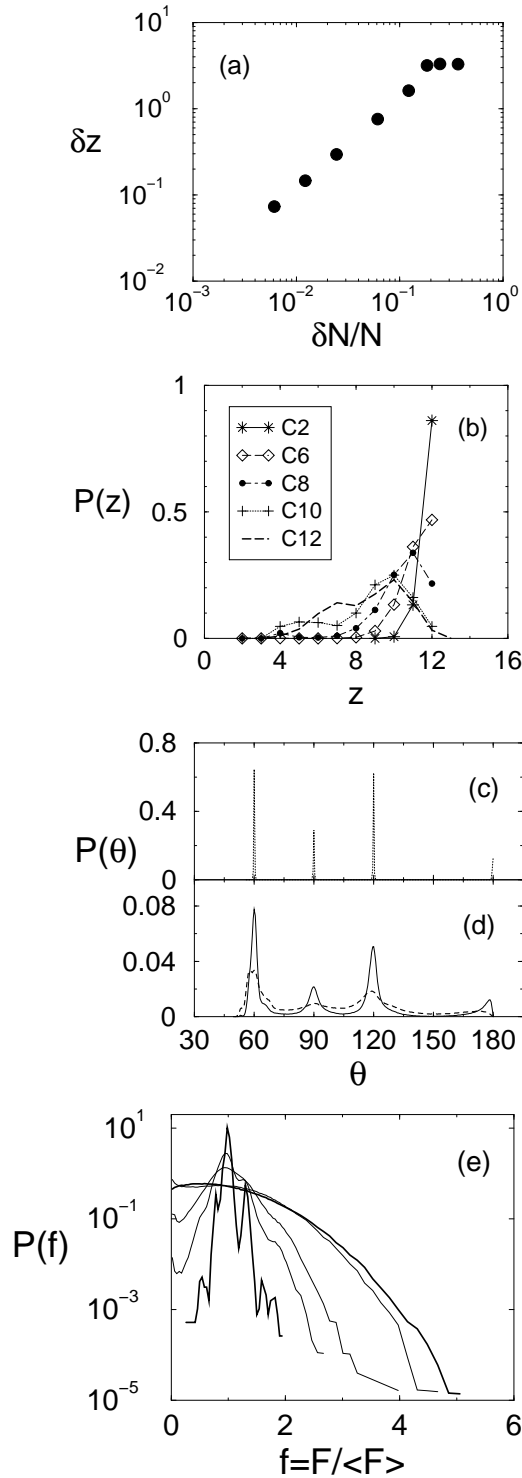


FIG. 6: Protocol (ii): In, (a) the relative change in the coordination number with respect to the initial monodisperse fcc array, as the fraction,  $\delta N$ , of particles are made bidisperse. (b) Coordination number distributions  $P(z)$ , for different amounts of disorder at fixed  $\phi = 0.742$ . Increasing configuration label corresponds to increasing disorder.  $P(\theta)$  for, (c) C6, and (d) C10 (solid line) and C12 (dashed). (e)  $P(f)$  over a range of disorder. The inner thick solid line is C2 and the outer thick line is C12.

On comparing the results for protocol (i) (Figs. 1 - 5), with those of protocol (ii) in Fig. 6, it appears that protocol (ii) leads to a more gradual change in the structure, compared with protocol (i). For (i), there is a much more dramatic change in structure between C10 and C12, than for the case of (ii). Still, the general trends remain similar, particularly for  $P(f)$ .

To provide a comparison with the quenched periodic packings already presented, results for gravity-sedimented, frictionless spheres of protocol (iii), are shown in Fig. 7. There are a number of subtle differences between the coordination number and force distributions between protocols (i),(ii) and protocol (iii). These differences primarily arise as a result of two effects. Firstly, the gravity packings are not periodic in all three directions, so surface effects play a role. Secondly, the gravity packings are able to adjust their packing fractions with increasing disorder, as shown in Fig. 7(a), whereas the fully periodic systems are at a fixed packing fraction. However, the generic features of the  $P(z)$  (Fig. 7(b)) and  $P(f)$  (Fig. 7(c)) distributions are similar. As more disorder is introduced into the lattice structure, the distributions broaden. In the case of  $P(f)$ , the high- $f$  tail becomes increasingly exponential. Thus, the fully periodic systems capture the essential features of the more realistic gravity packings.

The recent focus on  $P(f)$  has been emphasised due to suggestions that particular properties of  $P(f)$  can be used to signal the onset of glassiness in a glass-forming system, and likewise, the approach of the *jammed*, static state in a granular material or dispersion [16]. The concept being that the development of a peak in  $P(f)$ , for  $f < 1$ , represents the balance of forces required for mechanical stability into the jammed state - development of a yield stress. For finite-temperature systems, the jamming transition of purely repulsive, particles is accompanied by the development of a peak in  $P(f)$  at small  $f$ , as the temperature is lowered through the glass transition temperature [17]. (This picture is not so clear for the case of systems with longer-range attractive forces, as in Lennard-Jones systems [18, 19].) At zero-temperature, the peak in  $P(f)$  flattens into a plateau as the density of a jammed packing is lowered towards the jamming transition packing fraction [14, 20]. Therefore, for purely-repulsive, finite-range interactions, this jamming picture seems to apply.

In Fig. 8, results are shown for two jammed states of purely-repulsive systems, each with  $N = 256000$  particles. One configuration was generated using a fast molecular dynamics quench, from a high (liquid) temperature to  $T = 0$ . The other is a partially melted crystal quenched back down to  $T = 0$ . Despite the fact that not only are both of these systems jammed and that the  $P(f)$  curves in Fig. 8(a) sit on top of one another, differences in their structures are evident from the radial distribution function  $g(r)$  and  $P(\theta)$  of Figs. 8(b) and (c). This highlights the fact that amorphous and quasi-ordered systems can exhibit similar features in the jammed state.

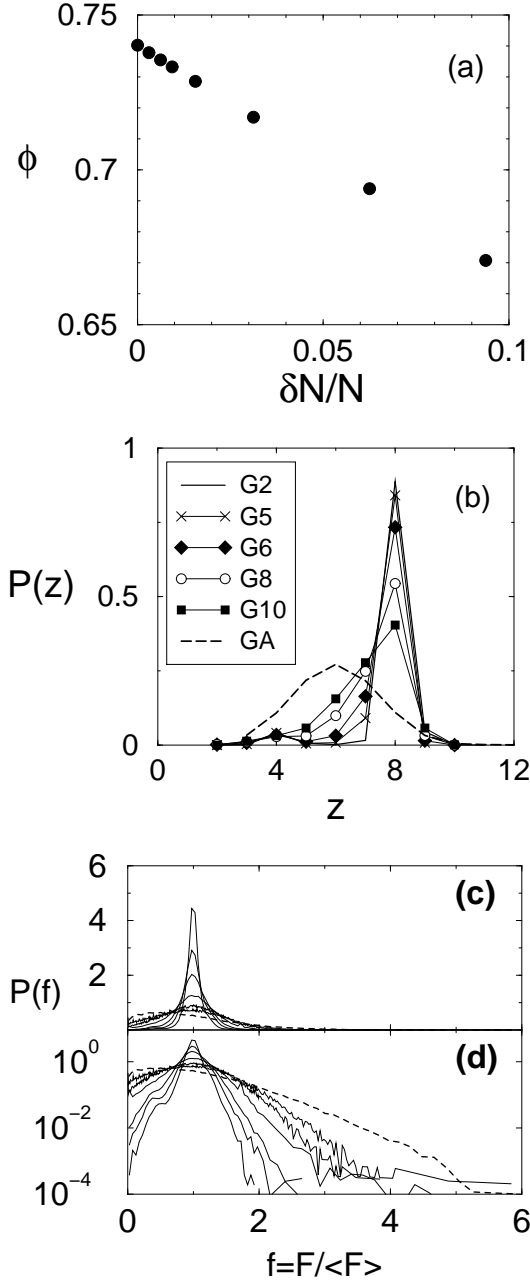


FIG. 7: Protocol (iii): Gravity sedimented packings. (a) Dependence of the depth-averaged packing fraction  $\phi$ , on  $\delta N$ . (b) Coordination number distributions  $P(z)$ , for different configurations, labelled with increasing disorder. Configuration  $GA$  is an amorphous packing, with a packing fraction close to the random close packing value  $\approx 0.64$ . (c) and (d) are the distributions of normal contact forces  $P(f)$ , for varying disorder on linear axes and linear-log respectively. The thick dashed line is  $GA$ .

Increasing disorder affects the mechanical properties of the packings subject to external perturbations [21]. Yet, for small amounts of disorder, one expects the configurations to vary only slightly in their properties from the

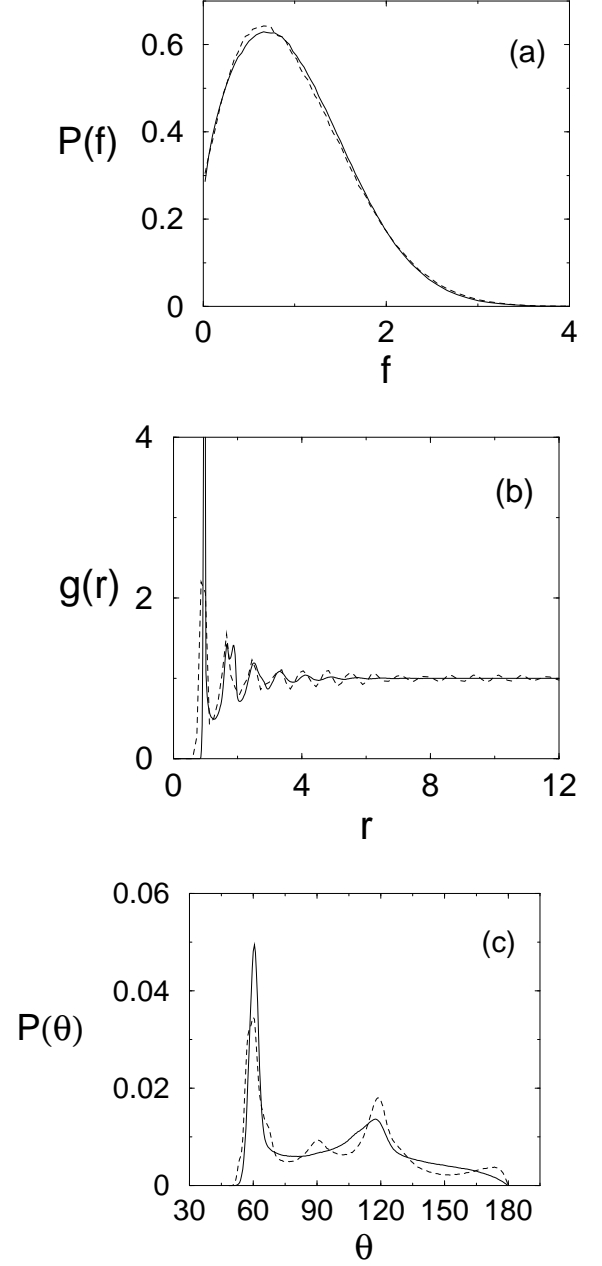


FIG. 8: (a) The distribution of contact forces  $P(f)$  for purely-repulsive, soft-spheres at  $T = 0$  and  $\phi = 0.742$ , with different histories. Soft-sphere glass (solid line) and partially melted crystal (dashed line). From  $P(f)$  and visualisation of the force networks, both configurations appear very similar. Structural measures show, however, that the partially melted crystal is significantly more ordered than the glassy state: (b) The radial distribution function,  $g(r)$ , shows long-range oscillations and, (c) the three-particle contact angle distribution  $P(\theta)$ , contains additional structure indicative of ordering.

underlying crystal. This is, indeed, the case, as described by Eq. 2. To determine how the disorder influences the dynamical properties of the packings, the low-frequency portion of the “phonon” density of states  $\mathcal{D}(\omega)$ , were ex-

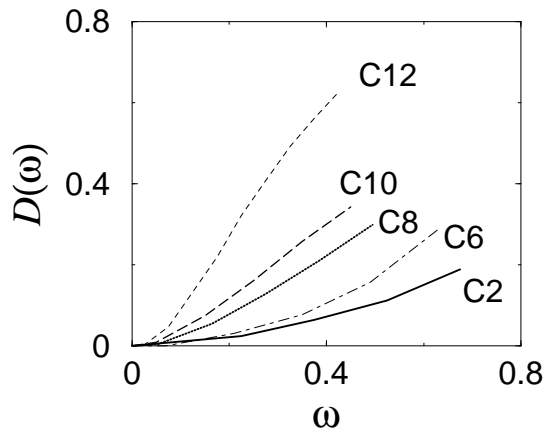


FIG. 9: Distribution of the vibrational normal modes of frequency  $\omega$  - the density of states -  $\mathcal{D}(\omega)$ , for the quenched packings of protocol (i). Only, the low- $\omega$  region of the distribution is shown. With increasing disorder, the number of low-frequency modes increases relative to the fcc lattice.

tracted for the  $N = 16384$  systems [22]. Figure 9 shows  $\mathcal{D}(\omega)$  as a function of frequency  $\omega$ , for configurations with varying amounts of disorder. Increasing disorder leads to an increasing population of the low- $\omega$  region in  $\mathcal{D}(\omega)$ , not unlike lattice-disorder models [23, 24].

The relation, Eq. 2, provides a useful measure of the disorder, when the disorder is weak. Figure 10 shows that over this same range in  $\delta z$ , where the configurations are not too different from the original lattice, many of the packings' properties scale. In particular, *relative to the crystal state*, the lowest normal mode frequency varies approximately linearly with coordination number. This is reminiscent of the way jammed amorphous packings behave as the density is lowered towards the random close packing point from above [25, 26]. It is suggestive, therefore, that there may exist a characteristic length scale associated with the increasing disorder, though, as yet, one has not been identified here.

In conclusion, the effect of structure on the properties of static packings has been studied. Structure plays a dramatic role in modifying the distribution of normal contact forces  $P(f)$  of frictionless particle assemblies, from an initial delta-function, for the face-centred cubic array, to the more familiar 'exponential' decay, with finite disorder. Likewise, the distributions of the coordination number broaden quickly. These two findings may, in part, explain the reason why it has been difficult to *experimentally* observe any significant dependence of  $P(f)$  on structure [9]. Even a relatively small number of defects can broaden  $P(f)$  quite substantially.

Dynamical properties of the packings have been investigated by extracting statistics on the lowest-lying normal modes. As more disorder is imposed, there is an increase in the density of states,  $\mathcal{D}(\omega)$ , at small frequency,  $\omega$ . Provided the structure remains close to the underlying lattice, the change in the coordination number relative to

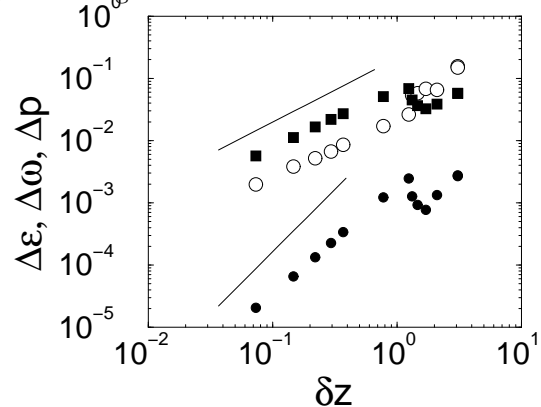


FIG. 10: Lowest normal mode frequency  $\Delta\omega$  (open circles), pressure  $\Delta p$  (solid squares), and contact energy  $\Delta\epsilon$  (solid circles), relative to the original fcc values, as a function of the degree of disorder, measured by  $\delta z$ . The solid lines are power-laws with exponents one and two.

the original lattice provides a useful measure of the disorder. When the disorder is weak, vis-a-vis Eq. 2, the value of the lowest-lying normal mode frequency scales approximately linearly with the disorder. It is somewhat amusing that these relationships are not too different from what is found in fully disordered packings near random close packing [27], where fractional changes in density play a similar role as disorder does here. Between these extremes of densely packed ordered arrays and loose amorphous packings, lies an intermediate regime that is not so well characterised. This intermediate regime retains a large degree of the contact topology of the original lattice, yet exhibits a strong degree of heterogeneity in the contact forces.

## Acknowledgments

I thank Moises Silbert for a critical reading of the manuscript. Part of this work was undertaken at the James Franck Institute, University of Chicago, with grant support from Grant Nos. NSF-DMR-0087349, DE-FG02-03ER46087, NSF-DMR-0089081, and DE-FG02-03ER46088, and is gratefully acknowledged.

- 
- [1] J. D. Bernal, Proc. Roy. Soc. Lond. A **280**, 299 (1964).
  - [2] A. Coniglio, A. Fierro, H. J. Herrmann, and

M. Nicodemi, eds., *Unifying Concepts in Granular Media and Glasses* (Elsevier, Amsterdam, 2004).

- [3] The nature of the decay of the tail to  $P(f)$  actually depends on how compressed the packing is [14, 20].
- [4] C. h. Liu, S. R. Nagel, D. A. Schecter, S. N. Coppersmith, S. Majumdar, O. Narayan, and T. A. Witten, *Science* **269**, 513 (1995).
- [5] D. M. Mueth, H. M. Jaeger, and S. R. Nagel, *Phys. Rev. E* **57**, 3164 (1998).
- [6] G. Lovoll, K. J. Maloy, and E. G. Flekkoy, *Phys. Rev. E* **60**, 5872 (1999).
- [7] F. Radjai, S. Roux, and J.-J. Moreau, *CHAOS* **9**, 544 (1999).
- [8] L. E. Silbert, G. S. Grest, and J. W. Landry, *Phys. Rev. E* **66**, 061303 (2002).
- [9] D. L. Blair, N. W. Mueggenburg, A. H. Marshall, H. M. Jaeger, and S. R. Nagel, *Phys. Rev. E* **63**, 041304 (2001).
- [10] J. M. Erikson, N. W. Mueggenburg, H. M. Jaeger, and S. R. Nagel, *Phys. Rev. E* **66**, 040301(R) (2002).
- [11] L. E. Silbert, D. Ertas, G. S. Grest, T. C. Halsey, and D. Levine, *Phys. Rev. E* **65**, 031304 (2002).
- [12] A. Donev, S. Torquato, and F. H. Stillinger, *Phys. Rev. E* **71**, 011105 (2005).
- [13] W. H. Press, B. P. Flannery, S. A. Teukolsky, and W. T. Vetterling, *Numerical Recipes in Fortran 77* (Cambridge University Press, New York, 1986).
- [14] L. E. Silbert, A. J. Liu, and S. R. Nagel, *Phys. Rev. E* **73**, 041304 (2006).
- [15] For the largest amount of disorder, there is a non-monotonic feature in the sense that the tail of  $P(f)$  appears more Gaussian (decays more rapidly) at these high compressions. If the pressure, or packing fraction, of the amorphous packing was subsequently decreased, the high- $f$  tail would again become increasingly exponential and is the reason for the differences between the circles and dot-dash line in Fig. 5(b). See [3].
- [16] C. S. O'Hern, S. A. Langer, A. J. Liu, and S. R. Nagel, *Phys. Rev. Lett.* **88**, 075507 (2002).
- [17] C. S. O'Hern, S. A. Langer, A. J. Liu, and S. R. Nagel, *Phys. Rev. Lett.* **86**, 111 (2001).
- [18] N. Lacevic and S. C. Glotzer, *J. Phys. Chem. B* **108**, 19623 (2004).
- [19] S. S. Ashwin, Y. Brumer, D. R. Reichman, and S. Sastry, *J. Phys. Chem. B* **108**, 19703 (2004).
- [20] H. A. Makse, D. L. Johnson, and L. M. Schwartz, *Phys. Rev. Lett.* **84**, 4160 (2000).
- [21] L. E. Silbert, in *Powders and Grains 2005*, edited by R. Garcia-Rojo, H. Herrmann, and S. McNamara (A.A. Balkema, Rotterdam, 2005).
- [22] <http://www.caam.rice.edu/software/ARPACK/>.
- [23] W. Schirmacher, G. Diezemann, and C. Ganter, *Phys. Rev. Lett.* **81**, 136 (1998).
- [24] S. N. Taraskin, Y. L. Loh, G. Natarajan, and S. R. Elliott, *Phys. Rev. Lett.* **86**, 1255 (2001).
- [25] L. E. Silbert, A. J. Liu, and S. R. Nagel, *Phys. Rev. Lett.* **95**, 098301 (2005).
- [26] M. Wyart, S. R. Nagel, and T. A. Witten, *Europhys. Lett.* **72**, 486 (2005).
- [27] M. Wyart, L. E. Silbert, S. R. Nagel, and T. A. Witten, *Phys. Rev. E* **72**, 051306 (2005).